



## RESEARCH ARTICLE

# Trajectories of brain entropy across lifetime estimated by resting state functional magnetic resonance imaging

Yan Niu<sup>1</sup> | Jie Sun<sup>1</sup>  | Bin Wang<sup>1</sup>  | Yanli Yang<sup>1</sup> | Xin Wen<sup>2</sup> | Jie Xiang<sup>1</sup>

<sup>1</sup>College of Information and Computer, Taiyuan University of Technology, Taiyuan, China

<sup>2</sup>College of Software, Taiyuan University of Technology, Taiyuan, China

**Correspondence**

Jie Xiang, College of Information and Computer, Taiyuan University of Technology, Taiyuan, China.

Email: [xiangjie@tyut.edu.cn](mailto:xiangjie@tyut.edu.cn)

**Funding information**

the National Key R & D Program of China, Grant/Award Number: 2018AAA0102601; the National Natural Science Functional of China, Grant/Award Numbers: 61873178, 61876124, 61906130, 62176177; the Shanxi Province Application Basic Research Plan, Grant/Award Numbers: 20210302123099, 20210302124550; the Shanxi Provincial International Cooperation Foundation, Grant/Award Number: 201803D421047

**Abstract**

The human brain is a complex system of interconnected brain regions that form functional networks with differing roles in cognition and behavior. However, the trajectories of these functional networks across development are unclear and designing a metric to track the complex trajectory of these characteristics throughout the lifespan is challenging. Here, permutation entropy (PE) was used to examine age-related variations in functional magnetic resonance imaging (fMRI) in healthy subjects aged 6–85 from global, network, and nodal perspectives. The global PE followed an inverted U-shaped trajectory that peaked at approximately age 40. The trajectory of the motor and somatosensory functional network was more consistent with a linear model and increased with age; other functional networks showed inverted U-shaped trajectories that peaked between 25 and 52 years of age. All nodes showed inverted U-shaped trajectories. Using cluster analysis, the peak ages of nodes were grouped into three clusters (at 24, 38, and 51 years). Overall, we characterized four aging trajectories: networks with a linear increase, early peak age, intermediate peak age, and older peak age. These findings suggest possible complexity in trajectories at critical age points regarding changes in related functional brain networks.

**KEYWORDS**

aging, fMRI, permutation entropy, U-shaped trajectory

## 1 | INTRODUCTION

The human brain is an extremely complex system, and with increasing age, a series of changes occur in the understanding and processing of complex information. The lifespan of healthy individuals is characterized by continuous changes in brain complexity throughout childhood, youth, middle age, and old age that follow specific maturation patterns. The lifetime trajectory of brain complexity has been studied: some studies suggest a linear decline from early ages (Fjell

et al., 2013; Goodro et al., 2012), while others have reported a quadratic trajectory, with an increase followed by a decrease (Gutchess, 2014; Karl et al., 2017; Potvin et al., 2016); alternatively, other studies have reported a cubic relationship (Fjell et al., 2013; Potvin et al., 2016). These changes are structurally reflected with increased white matter (WM) volume and an inverted U-shaped change in gray matter (GM) volume in developing children and adolescents (Giedd et al., 1999). Upon maturity, both WM and GM volumes degenerate with healthy aging (Djma et al., 2012; Sowell et al., 2003). Changes in brain structure are associated with functional changes and are accompanied by reduced brain activity (Fjell & Walhovd, 2010).

Yan Niu and Jie Sun are the co-first authors.

This is an open access article under the terms of the [Creative Commons Attribution-NonCommercial-NoDerivs](https://creativecommons.org/licenses/by-nc-nd/4.0/) License, which permits use and distribution in any medium, provided the original work is properly cited, the use is non-commercial and no modifications or adaptations are made.

© 2022 The Authors. *Human Brain Mapping* published by Wiley Periodicals LLC.

Previous studies have analyzed these changes in terms of functional connectivity (FC) (Liu et al., 2021; Yan et al., 2018), graph theory (Jezga et al., 2020; Yan et al., 2018), and network efficiency (Zhao et al., 2017). Studies have found that local efficiency decreases linearly from adulthood to old age, while global efficiency remains unchanged. In Achard et al.'s (Achard & Bullmore, 2007) analysis of the brain connection network, elderly individuals had lower topological efficiency of spontaneous functional networks in a resting state. Designing a metric to track the complex trajectory of these characteristics throughout the lifespan from a functional network perspective is challenging but would establish a foundation for understanding complex systems in the human brain.

Studying the nonlinear dynamics of brain signals during development by using the complexity index is not ideal. The complexity index represents the variability in the information processing ability of the brain (Yang et al., 2018). A large number of researchers have used advanced neuroimaging techniques to conduct noninvasive studies with elderly individuals (Chen et al., 2019; Wang et al., 2020); however, few subjects were assessed in these studies, and age-related changes in different brain regions remain unknown. For example, Fenne Margreth Smits et al. (2016) studied electroencephalography (EEG) signals from 41 healthy subjects aged 18–85 and found that a parabola was the best fitting curve for modeling the Higuchi fractal dimension of age. Entropy is a widely used complexity measure that has the advantages of strong noise resistance, a stable algorithm and high retest reliability (Sun et al., 2020; Yang et al., 2018). The higher the value of entropy is, the greater the information processing capacity and functional development of the brain. Reduced brain activity means that the central nervous system is less flexible and efficient in processing information. Previous studies have reported that quadratic regression models can fit developmental trajectories more accurately than linear models, but linear models are still used in most studies. Shumbayawonda et al., (2019) used entropy measures to assess magnetoencephalography (MEG) signals and found that age had a significant impact on complexity in five brain regions. Moses O. Sokunbi et al. (2015) demonstrated that whole-brain mean fuzzy approximate entropy (fApEn) was significantly negatively correlated with age using a resting-state functional magnetic resonance imaging (fMRI) data set from 86 healthy adults.

Based on the above studies, some advances have been made in understanding the structural and functional changes in healthy aging, but the trajectory of functional brain networks remains unclear. Permutation entropy (PE) is a method to measure uncertainty in dynamic time series (Bandt & Pompe, 2002). PE considers only the grade of the samples, not their metrics. As it is a sequential measure, PE has some advantages over other commonly used entropy measures, including simplicity, low computational complexity without additional model assumptions, and robustness in the presence of observed and dynamic noise. PE has been used in EEG studies of human absence epilepsy (Ferlazzo et al., 2014), typical absence seizures (Jing et al., 2014), and mild cognitive impairment (MCI) (Timothy et al., 2014). These studies have suggested that PE is a useful tool for studying brain complexity.

In this study, we used PE approaches to examine age-related alterations in a large cohort of 319 healthy subjects ranging from 6 to 85 years old to explore trajectories of brain development. At a system level, we aimed to determine age-related trajectories of brain development from global, network, and nodal perspectives to provide a complete understanding of the topological changes in PE with age.

## 2 | MATERIALS AND METHODS

### 2.1 | Data availability statement

This study included data from 319 healthy individuals (age range, 6–85 years; mean age,  $39.5 \pm 45.5$  years) from the NKI/Rockland Sample (NKI-RS), which was provided by the Nathan Kline Institute (NKI, NY) and is publicly available online in the International Neuroimaging Data-sharing Initiative (INDI) database ([http://fcon\\_1000.projects.nitrc.org/indi/enhanced/mri\\_protocol.html](http://fcon_1000.projects.nitrc.org/indi/enhanced/mri_protocol.html)). The NKI Institutional Review Board approved the research protocol to collect and share the data.

### 2.2 | Data acquisition and preprocessing

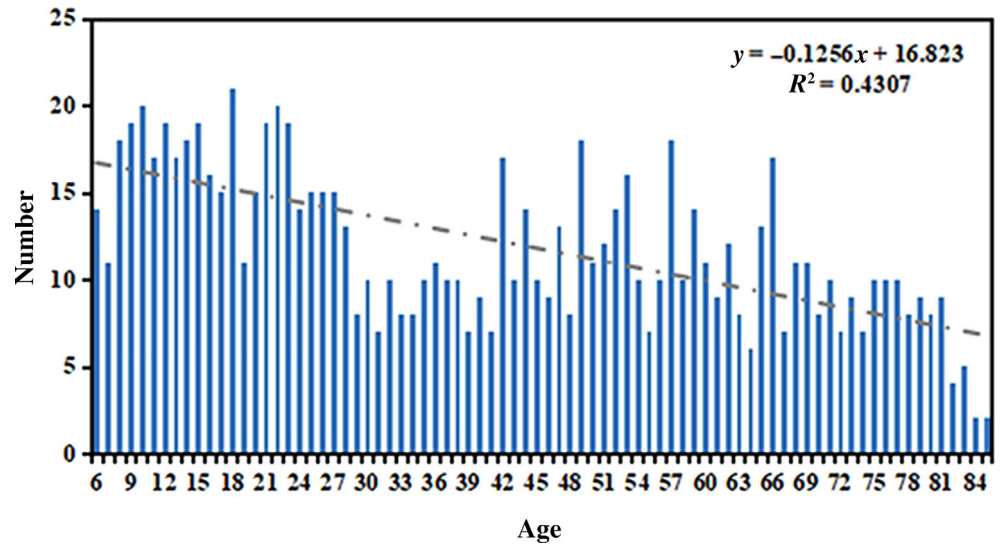
All participants were scanned with a SIEMENS MAGNETOM TrioTim syngo MR B17 using the following parameters: repetition time (TR)/echo time (TE) = 645/30 ms, time point = 900, field of view (FOV) =  $222 \times 222$  mm<sup>2</sup>, and slice number = 40. Figure 1 shows the distribution of subjects' ages. Further details regarding the acquisition protocol of the study images are available on the INDI website.

The Data Processing Assistant for Resting-State fMRI (DPARSF v2.3) software (Yan & Zang, 2010) package, which is based on two software packages, Statistical Parametric Mapping 8 (SPM 8) (<http://www.fil.ion.ucl.ac.uk/spm>) and RS-fMRI Data Analysis Toolkit 1.8 (REST 1.8) (Song et al., 2011) was used, and the images were analyzed on the MATLAB 2014a platform. Briefly, the preprocessing steps were as follows: the first 10 volumes of the functional images during the participant's habituation to the imaging process were discarded; slice-timing correction was performed based on the last slice; the images were realigned to compensate for head movement using a six-parameter rigid-body spatial transformation because excessive head motion may induce large artifacts in fMRI time series; the images were normalized to the Montreal Neurological Institute (MNI) space; and the signal drift was removed using a linear model. Additionally, spatial smoothing of the brain PE maps was performed to reduce the white noise and suppress the effects due to residual differences during intersubject averaging using an 8-mm full-width at half-maximum (FWHM) smoothing kernel.

### 2.3 | Entropy algorithms

Step 1: Given a time series of length  $N$ :

**FIGURE 1** The distribution map of the subject age. We first assumed the ribbon distribution, found the linear regression equation and the correlation coefficient  $r$ . It is seen from the figure that  $r = .65$ , which approximately fits with a uniform distribution.



$$X = \{x(1), x(2), \dots, x(N)\} \quad (1)$$

Step 2: The  $pm$  dimensional phase space reconstruction of raw data by serial number is:

$$X(i) = [x(i), x(i + \tau), \dots, x(i + (pm - 1)\tau)], i = 1, 2, \dots, N - (pm - 1)\tau \quad (2)$$

where  $pm$  is the embedding dimension and  $\tau$  is the delay time.

Step 3: Each reconstructed component is then rearranged in ascending numerical order:

$$x(i + (j_1 - 1)\tau) \leq x(i + (j_2 - 1)\tau) \leq \dots \leq x(i + (j_{pm} - 1)\tau) \quad (3)$$

where  $j_1, j_2, \dots, j_{pm}$  represents an index of the columns of each element in the reconstructed component.

If two values are equal, for example:

$$x(i + (j_1 - 1)\tau) = x(i + (j_2 - 1)\tau) \quad (4)$$

They are ordered according to the size of the  $j_1$  and  $j_2$  values; when  $j_1 < j_2$ :

$$x(i + (j_1 - 1)\tau) < x(i + (j_2 - 1)\tau) \quad (5)$$

Step 4: We can thus obtain a set of symbol sequences by each row of the reconstructed matrix of any time series, where the symbol sequences are as follows:

$$s(g) = (j_1, j_2, \dots, j_{pm}), g = 1, 2, \dots, k, k \leq pm! \quad (6)$$

Step 5: There are  $pm!$  possible symbol sequences obtained by the  $pm$  dimension mapping;  $s(g)$  is only one of them. The probability of occurrence of the various permutations,  $P_1, P_2, \dots, P_k$ , can be calculated and the permutation entropy is defined as follows:

$$PE(N, pm, \tau) = - \sum_{j=1}^k P_j \ln P_j \quad (7)$$

Three parameter values must be set when calculating PE: the length  $N$  of the time series, embedding dimension  $pm$ , and time delay  $\tau$ . The magnitude of the PE represents the degree of randomness in the time series: smaller values indicate that the time series is more regular and larger values indicate that the time series is more random. If the value of  $m$  is too large, the phase space reconstruction will homogenize the time series, and the subtle changes in the sequence will not be reflected. To meet this condition, we set  $m = 4$  and  $\tau = 1$  (Jing et al., 2014).

## 2.4 | Power template

A recent study showed that the power template can better define nodes and has higher retest reliability for whole-brain and local networks than anatomical automatic labeling templates and other templates; therefore, we used the power template in this study. The 10 networks included the power template were as follows: the motor and somatosensory network (SMN), cingulo-opercular network (CON), auditory network (AN), default mode network (DMN), visual network (VN), frontoparietal network (FPN), salience network (SN), subcortical network (SCN), ventral attention network (VAN), and dorsal attention network (DAN) (Power et al., 2011).

## 2.5 | Cluster analysis

The core idea of the clustering analysis algorithm is to divide data objects into different clusters through iteration to minimize the objective function and to make the generated clusters as compact and independent as possible. The algorithm steps were as follows:

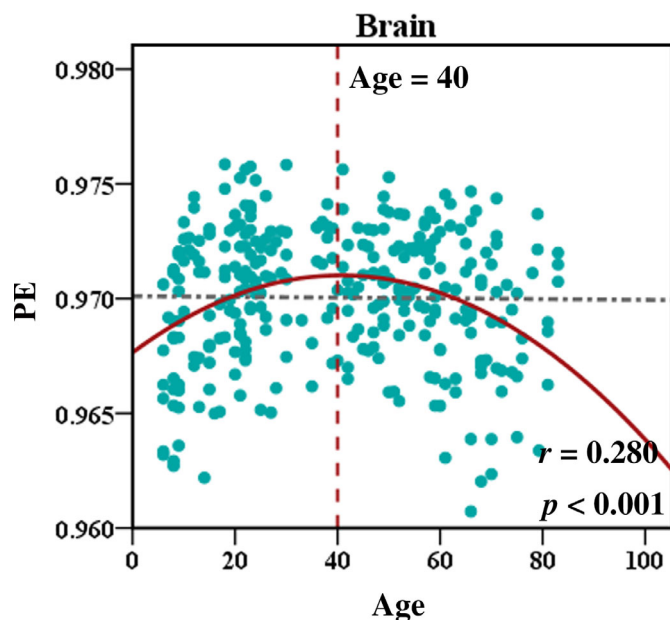


**FIGURE 2** The developmental trajectory of the global brain. Global human brain developmental trajectory; black represents the linear model, and red represents the quadratic regression model. The entropy of the global human brain throughout its lifecycle shows an inverted U-shaped trajectory with increasing age ( $r = .28$ ,  $p < .001$ ).

(1) randomly select  $k$  objects as the centroids of the initial  $K$  clusters; (2) assign the remaining objects to the nearest cluster based on their distance from the centroid of each cluster and identify the centroid of the newly formed cluster; and (3) repeat this iterative relocation process until the objective function is minimized.

In this article, the PE of 264 nodes in the power-264 template was calculated, and the trajectory characteristics of each node were determined after regression analysis of the obtained entropy. The  $k$ -means clustering method was used to cluster the 264 resulting trajectories, and finally, three cluster centers were obtained.

## 2.6 | Statistical analysis

The DPARSF toolbox was used to define the regions of interest (ROIs) from the power-264 template to extract the average PE values based on the peak MNI coordinates (XYZ), and the radius of the spheres was set to 8 mm. All statistical analyses were performed using Statistical Package for Social Science (SPSS) version 20 (<http://www.spss.com/>). A linear model and quadratic regression model were used to fit the PE developmental trajectory during aging. We applied the false discovery rate (FDR) to correct for multiple comparisons. We used cluster analysis to classify regression curve patterns in the nodes. Considering the potential impact of cerebrospinal fluid and gray matter volume on the experiment, we calculated the CSF and GM volumes for each subject and input them as covariates using SPSS to evaluate changes in brain entropy with age. The results indicated that the  $p$ -values of the CSF and GM volumes were .856 and .449, respectively, indicating that there was no significant effect.

## 3 | RESULTS

### 3.1 | Global PE trajectory

We observed the lifetime global brain trajectory, which exhibited an inverted U-shaped trajectory with age ( $r = .28$ ,  $p < .001$ ) (Figure 2). PE in the global brain peaked at approximately age 40, suggesting that this age is an important time point for maturation and degeneration of the human brain. Of the nodal peaks, 105 of the 264 regions exhibited nonlinear changes with age ( $p < .001$ , Bonferroni correction).

### 3.2 | Network PE trajectory

We further investigated the age-related changes in network trajectories. The PE in the SMN was more consistent with the linear model that showed an increase with age ( $r = .161$ ,  $p = .012$ ) (Figure 3). The PE in the other networks (CON, AN, DMN, VN, FPN, SN, SCN, VAN, and DAN) was more consistent with the quadratic regression model that exhibited an inverted U-shaped trajectory, with the networks peaking at 34, 34, 41, 32, 45, 42, 25, 38, and 52 years, respectively (Figure 3).

The nodal peak in the networks exhibited nonlinear changes with age ( $p < .001$ , Bonferroni correction). Figure 4 shows the peak variation in the nodes in each network. With the exception of the nodal peaks in the DMN and SN, the nodal peaks in the other networks (CON, AN, VN, FPN, SCN, VAN, and DAN) were near the peaks of the networks.

### 3.3 | Nodal trajectories

We further investigated age-related changes in the nodes, all of which exhibited a nonlinear inverted U-shaped trajectory across the lifespan. The peak ages for individual nodes varied across brain areas and ranged from 17 to 62 years (Figure 5b). Notably, most of the regions with peaks at older ages were in the SMN, FPN, and DAN. Then, we used cluster analysis and found that the peak points of nodes were grouped into three clusters: Cluster 1 (23.5830, 0.9863), Cluster 2 (38.3830, 0.9910), and Cluster 3 (51.0339, 0.9901) (Figure 5a). Three key points during aging were obtained: 24, 38, and 51 years.

Subsequently, we classified the peaks of the nodes and calculated the proportion of each cluster in the different networks. As shown in Figure 6, all nodal peak points in the SMN were concentrated at approximately 51 years, which may be related to compensatory mechanisms in aging. In the AN, SCN, and VAN, all nodal peak points were concentrated at approximately 38 years, which indicated that these nodes were mature at approximately 38 years. In the CON, DMN, and SN, the nodal peaks were distributed among the three clusters, indicating that there were differences between the aging of networks and the aging of nodes. The nodal peaks in the FPN and DAN were

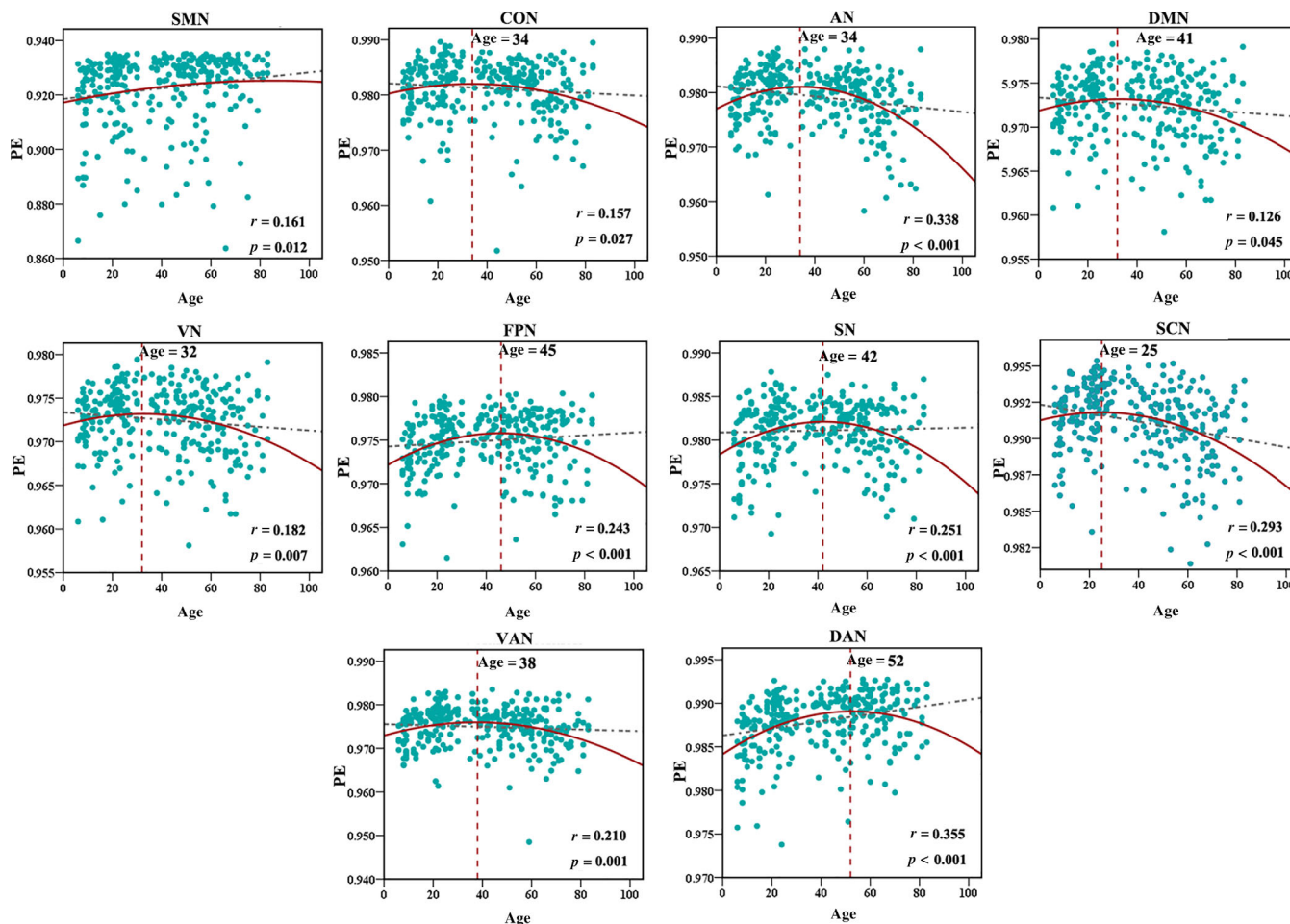


**FIGURE 3** The developmental trajectory of network trajectories. The black line represents the linear model, and the red line represents the quadratic regression model. The SMN was more consistent with the linear model, which increased with age ( $r^2 = .161$ ,  $p = .012$ ). The other networks (CON, AN, DMN, VN, FPN, SN, SCN, VAN, and DAN) were more consistent with the quadratic regression model and exhibited an inverted U-shaped trajectory with peaks at different ages.

distributed among two clusters (38 and 51 years). In the VN, the nodal peaks were distributed between two clusters (24 and 38 years).

Next, we further characterized the three clusters. In Figure 7, each color represents a different network. First, we studied Cluster 1 (peak at 24 years). Figure 7a-1 shows the proportions of the SN, VN, DMN, and CON in this cluster; the proportion of corresponding network nodes in the cluster were 12%, 25%, 25%, and 38%, respectively. Figure 7a-2 shows the locations of these networks in the whole brain. Then, we studied Cluster 2 (peak at 38 years). Figure 7b-1 shows the proportion of the networks (SN, AN, VN, DMN, DAN, VAN, FPN, SCN, and CON) in this cluster. Most nodes peaked at approximately 38 years. Notably, the largest proportion of nodes was from the DMN, at 26%. The locations of these networks are presented in Figure 7b-2. Finally, we studied Cluster 3 (peak at 51 years). Figure 7c-1 shows the proportion of the networks (DAN, SN, FPN, VN, CON, and SMN) in this cluster. The FPN and SMN accounted for 27% and 30%, respectively. The locations of these networks in the whole brain are shown in Figure 7c-2.

## 4 | DISCUSSION

In this study, we used PE approaches to examine age-related brain alterations in a cohort of healthy subjects ranging from 6 to 85 years old. We reached three conclusions. First, the global PE followed an inverted U-shaped trajectory with a peak age around age 40. Second, with the exception of the SMN (which was more consistent with a linear model and increased with age), most of the networks showed inverted U-shaped lifespan trajectories, with the peak ages for PE varying across networks (ranging from 25 to 52 years). Third, we further investigated age-related changes in the nodes, all of which showed inverted U-shaped lifespan trajectories, with the peak values across nodes ranging from 17 to 68 years. Finally, this study identified four basic aging trajectories: a functional network that exhibited a linear increase (i.e., the SMN); networks with an early peak age (<35 years) (i.e., the CON, VN, AN, and SCN); networks with a peak in middle age (35–44 years) (i.e., the DAN, SN, and VAN); and networks with an older peak age (>44 years) (i.e., the FPN and DAN).

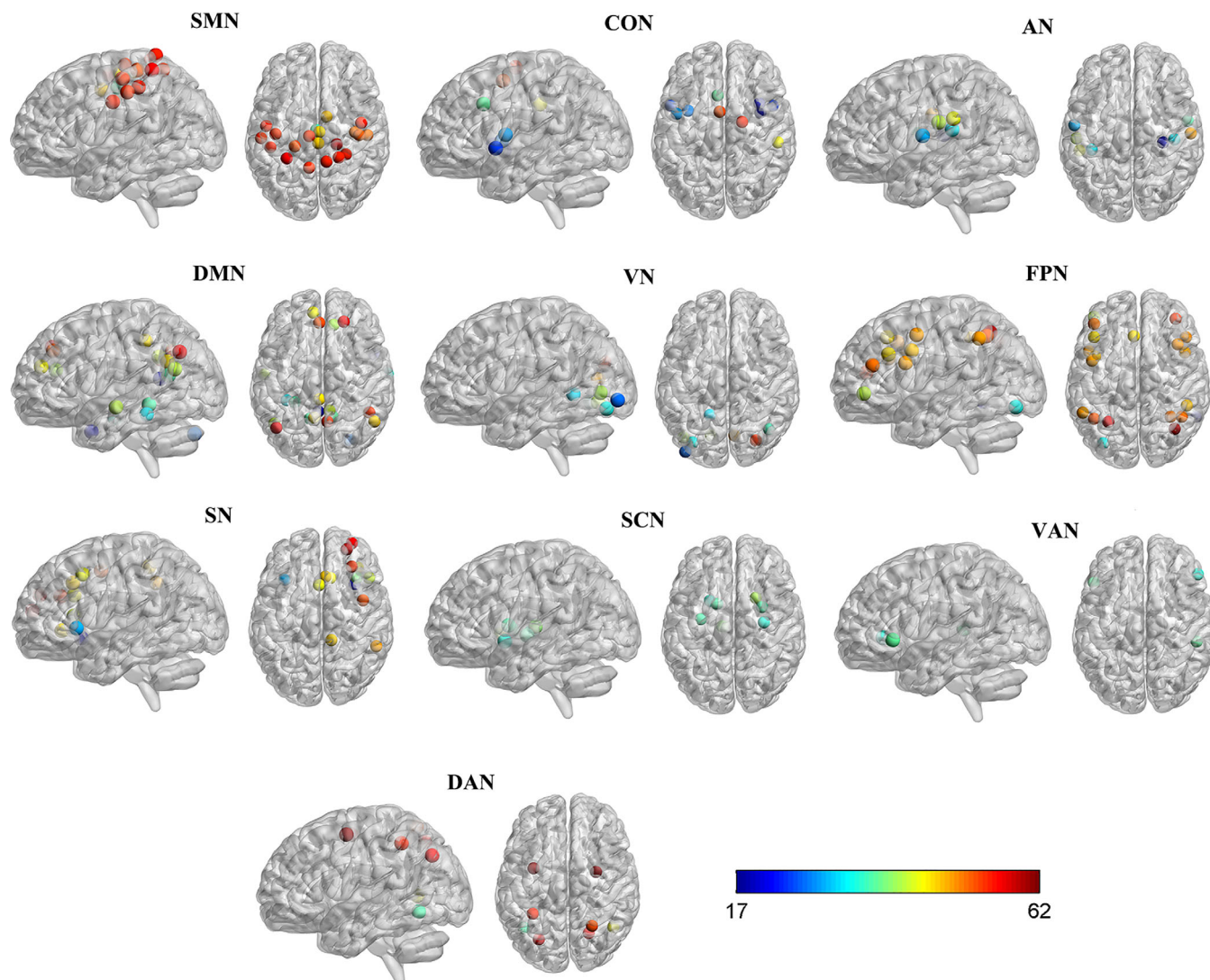


**FIGURE 4** The nodal peaks in 10 networks exhibited nonlinear changes with age ( $p < .001$ , Bonferroni correction). With the exception of nodal peaks in the DMN and SN, the nodal peaks in the other networks (CON, AN, VN, FPN, SCN, VAN, and DAN) are near the peaks of the whole networks.

#### 4.1 | Peak global brain development at age 40

We found that the global PE followed an inverted U-shaped trajectory with a peak age around age 40, suggesting that this age is an important time point for maturation and degeneration of the human brain. The whole brain showed deviations from linearity at critical ages, that is, the ages where estimated atrophy started to decelerate. This is consistent with human psychology and behavior. Psychological development in early childhood gradually matures, and the ability to handle events constantly improves. Middle age is a turning point in development; after this point, there is a decline in various brain functions, which manifests in cognition and behavior. Previous studies (Fjell et al., 2013; Zhixiong et al., 2016) have shown that the human brain peaks at approximately age 40, which is an important time point regarding degeneration of the brain. In childhood, memory and cognitive processing ability continuously improve, while in adulthood, they are relatively stable. The age of 40 is a turning point in development

when cognitive function begins to decline. This notion is consistent with our understanding of the cognitive function of the brain and the results of this article.

#### 4.2 | The inconsistency of the network peaks

Previous neuroimaging studies (Hasan et al., 2009; Kochunov et al., 2012) revealed different lifespan trajectories for different WM tracts, with peak ages varying from 20 to 40 years old (Djma et al., 2012; Yeatman et al., 2014). Many studies have shown a nonlinear relationship between the topological efficiency of the brain and the volume of WM and GM with age (Allen et al., 2005; Lupien et al., 2007), including a study with sample overlap (Walhovd et al., 2011). Since each network may be functionally inconsistent, the developmental trajectory of this network may also vary throughout the lifespan, leading to changes in peak points. Overall, these studies

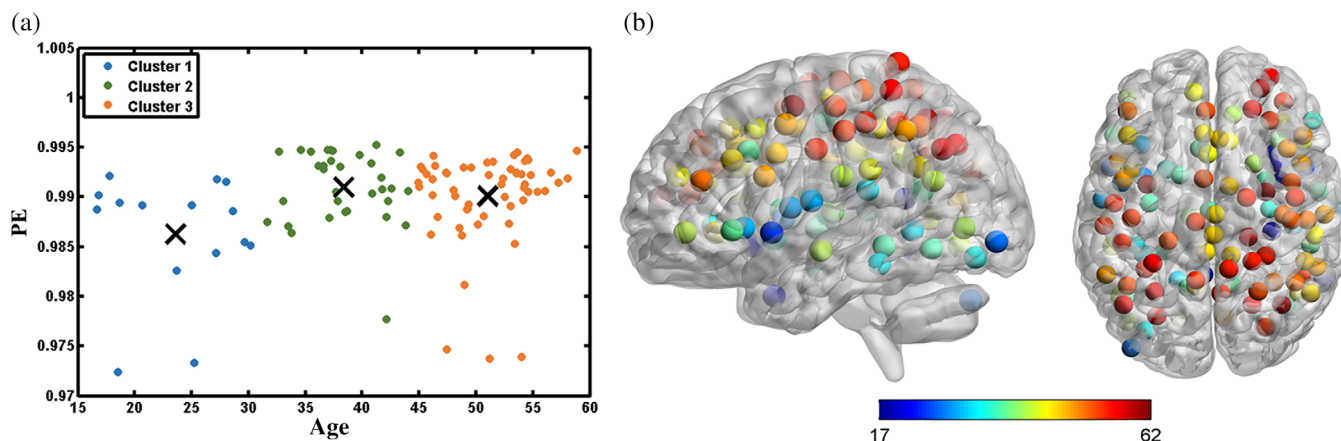
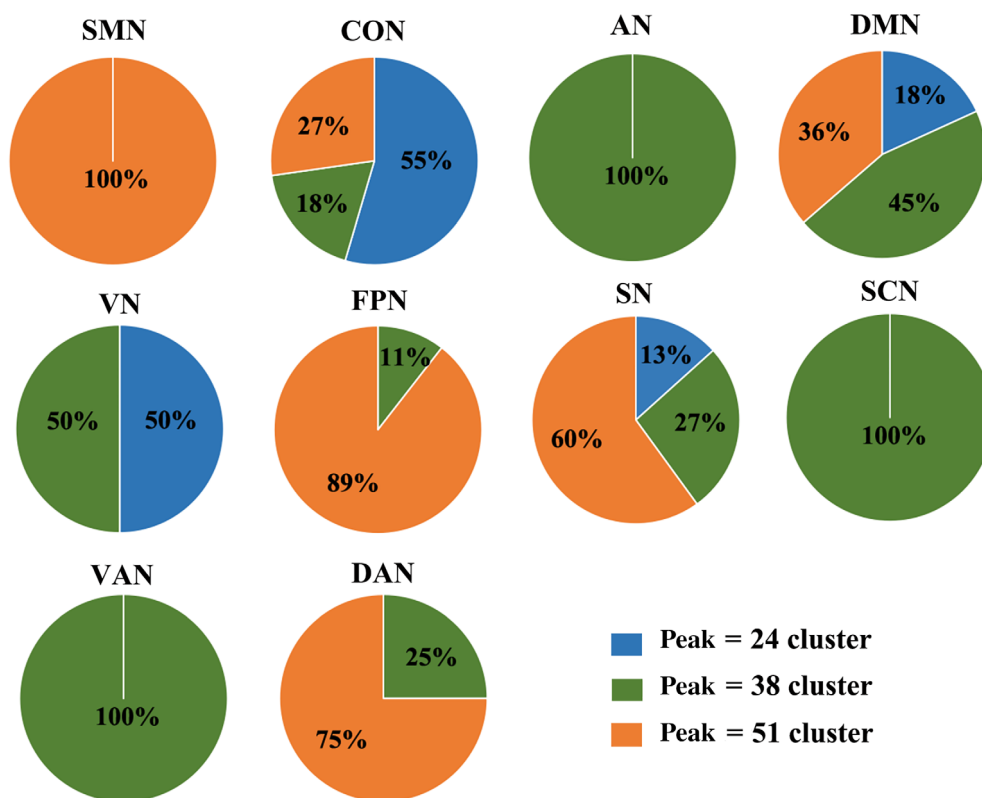


**FIGURE 5** The peak for each node and the clustering of node development trajectories divided into three clusters. (a) We used K-means cluster analysis and found that the peak points of the nodes were grouped into three clusters: Cluster 1 (23.5830, 0.9863), Cluster 2 (38.3830, 0.9910), and Cluster 3 (51.0339, 0.9901). (b) The nodal peak of human brain. A total of 105 of 264 regions exhibited nonlinear changes with age ( $p < .001$ , Bonferroni correction). The peak ages for nodal varied across areas, from 17 to 62 years.

**FIGURE 6** The proportion of each cluster in the different networks. We found that all nodal peak points in the SMN are concentrated at approximately age 51. In the AN, SCN, and VAN, all nodal peak points are concentrated at approximately age 38. In the CON, DMN, and SN, the nodal peaks are distributed among the three clusters. The nodal peaks in the FPN and DAN are distributed between two clusters (peak = 38 cluster and peak = 51 cluster). In the VN, the nodal peak is distributed between two clusters (peak = 24 cluster and peak = 38 cluster).



are largely consistent with our results; the inconsistencies may be due to differences in sample selection. Below, we discuss each network in detail.

### 4.3 | The SMN exhibits a linear increase with age

The trajectory of the SMN was more consistent with a linear model and showed increases with age. Sofie Heuninckx found a positive correlation between activation levels in the higher sensorimotor network

and motor abilities in elderly individuals (Heuninckx et al., 2008), which is consistent with our study. Functional imaging studies have shown that older people engage in more complex brain activities than young people when performing motor tasks. We believe that this age-related hyperactivity reflects a compensatory mechanism or dedifferentiation. Compensation refers to additional activation that can counteract age-related brain dysfunction, whereas dedifferentiation leads to activation of classic motor coordination regions but also activation of higher sensorimotor regions in elderly individuals (Yeatman et al., 2014). Although the trajectory of the SMN as a whole is more in

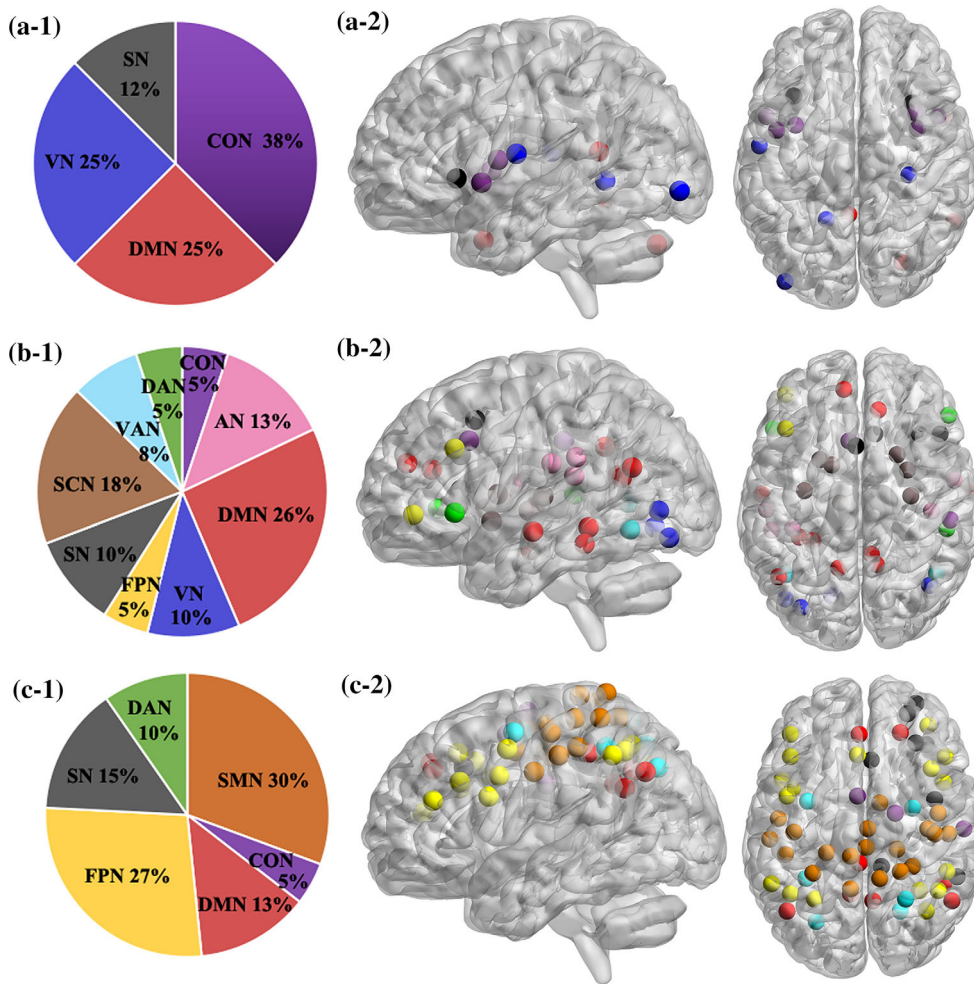


**FIGURE 7** The proportion of each network in the three clusters and location of the networks in the brain. Each color represents a different network. (a-1) The proportion of networks, such as SN, VN, DMN, and CON in peak = 24 cluster, with the proportion of nodes in these networks being 12%, 25%, 25%, and 38%. (a-2) shows the location of these networks in the brain of peak = 24 cluster. (b-1) shows the proportion of the networks (SN, AN, VN, DMN, DAN, VAN, FPN, SCN, and CON) in peak = 38 cluster. (b-2) The location of these networks of peak = 38 cluster. (c-1) The proportion of the networks (DAN, SN, FPN, VN, CON, and SMN) in peak = 51 cluster. (c-2) The location of these networks of peak = 51 cluster.

line with the linear model, the trajectory of the internal nodes was more in line with the inverted U-shape. The peak age of all nodes was late and concentrated in Cluster 3.

#### 4.4 | Peak primary sensory network maturation is at approximately age 30

The trajectories of the SCN, VN, and AN were more consistent with the quadratic regression model, which exhibits an inverted U-shape, and the PE in these networks peaked at 25, 32, and 34 years, respectively. Based on previous research findings (Zhixiong et al., 2016), the visual, auditory, and sensory cortices reach their peaks earliest and then exhibit a downward trend. The primary sensory brain network shows the fastest development. This is consistent with our results. The nodes in the SCN were all concentrated at approximately age 38, but the final peak age of the SCN as a whole was at approximately age 25. Thus, the peak age of the functional network as a whole was inconsistent with each node. This difference may be due to the process of calculating an average value for the functional network; additionally, nodes focus only on particular locations and therefore exhibit significant differences. In the AN, the overall peak age was essentially

the same age as each node in the network, which showed consistency. Based on previous studies, the causes of aging in the VN may be related to slower processing speed and reduced brain tissue volume in elderly individuals (Müller-Oehring et al., 2013). Regarding the subcortical functional network, changes in subcortical structures surrounded by myelinated neurons with long axons may be related to myelination (Ostby et al., 2009). Recent diffusion tensor imaging studies have confirmed that myelination is the main principle underlying late childhood and adolescent development (Giorgio et al., 2008; Lebel et al., 2008). The decrease in complexity may reflect the process of synaptic pruning (Huttenlocher, 1990). We found that the overall peak age of primary sensory networks was slightly earlier and concentrated at approximately 30 years old. The peak ages of the internal nodes were different from those of the whole networks, but most of the peaks of the aging nodes were concentrated in a certain range.

#### 4.5 | Peak control network development at approximately age 40

The trajectories of the CON and FPN were more consistent with the quadratic regression model, which exhibited an inverted U-shape.



These networks peaked at ages 34 and 45, respectively. The CON is involved in many complex physical and visceral motor functions and pain responses, while the posterior cingulate gyrus is the region that monitors sensory, stereotactic and memory functions. Some studies have shown that the peak ages for nodal efficiency vary across networks, and the peak age for CON efficiency was reported to be at approximately 40 years, which is slightly different from our study (Zhao et al., 2015). We think that this difference may be related to the selection of subjects and research methods. We found that the final peak age for this network was at approximately 34 years, but the nodes peaked at different ages. The peak age of the frontoparietal functional network was not exactly the same as reported in previous studies; however, the general scope was consistent with previous findings. For example, previous studies have found that aging of the frontal cortex begins at approximately 45 years old (Zhixiong et al., 2016), and Tengda Zhao et al. (2015) found that the peak value of the parietal lobe appeared later, at approximately 50 years. Regarding the frontoparietal functional network, the peaks in the prefrontal regions were consistent with the peak range reported for various cognitive measures, such as inductive reasoning, spatial visualization, episodic memory, and perceptual speed (Salthouse, 2009; Zhao et al., 2015), suggesting that the age-related adjustments in functional network organization may support alterations in cognitive abilities across the lifespan. Although the aging of nodes in the functional network was not completely consistent with the peak age of the whole network at age 45, the peak ages in most nodes were later, which was consistent with the overall peak age.

#### 4.6 | Peak DMN development at approximately age 41

The entropy in the DMN reached its peak at 41 years of age and then began to decline. Studies have shown that during normal aging, functional connectivity between the DMN in the anterior and posterior parts of the central axis of the brain changes (Zhixiong et al., 2016). From childhood to adulthood, the connection strength gradually increases, reaches a peak, and then shows a downward trend. In old age, the functional connectivity of the DMN is significantly weakened. This is reflected in the decline in cognitive abilities such as memory and attention. This functional change manifests in deficits, such as atrophy in the cerebral cortex, damage to WM integrity, abnormal dopamine neurotransmission, and amyloid deposition (Lindbergh et al., 2019; Sokunbi et al., 2013). We found that the nodal peak age in the DMN was distributed across the three clusters, while the whole network peaked at 45 years. This finding shows that the aging of the DMN varies rather than aging in unison.

#### 4.7 | Peak development of the attention networks

The attention networks included the VAN, SN, and DAN, and they peaked at 38, 42, and 52 years, respectively. The VAN is mainly driven

by bottom-up stimulation. Basic networks, such as those related to motor control, attention/cognitive control, conflict monitoring, social information processing and emotional management, develop in children and adolescents, consistent with a series of behavioral phenomena, such as children's "learning peak" and adolescents' "adolescence" (Liu et al., 2019; Zhixiong et al., 2016). Compared with adults, the functional connectivity of the VAN is weaker at younger ages. The nodes in the VAN all peaked at approximately age 38, and the final peak of the whole network was at approximately 38. Interestingly, the peak ages of the whole network and internal nodes were highly consistent. Both affective processing and executive function are linked to the brain's SN (Touroutoglou et al., 2018). As with the DMN, the peak age of the internal nodes in the SN was distributed across the three clusters, and the peak age of the whole network did not represent the peak age of each position in the network. The DAN provides top-down attention orientation, which matures later (Hoffmann, 2020). Although the peak age for the internal nodes varied in the middle-aged and elderly age groups, the peak age for most nodes was consistent with that of the whole network. These brain regions belong to the attention network; the peak ages of these brain regions were concentrated in a certain range and followed a hierarchical order. The peak ages of their internal nodes also followed hierarchical pattern. Therefore, although there was some internal consistency within brain areas during aging, the specific degree of aging in each brain region is different.

#### 4.8 | Comparison with existing research methods

Most previous studies in this area have constructed brain networks, and the resulting functional connectivity mainly focused on the synergy between nodes; in contrast, the entropy measurements applied in this study mainly start with the complex dynamics and focus on changes in that complexity in each node. Previous studies have analyzed these changes in terms of functional connectivity (FC) (Liu et al., 2021; Yan et al., 2018), graph theory (Jezga et al., 2020; Yan et al., 2018), and network efficiency (Liu et al., 2021; Yan et al., 2018; Zhao et al., 2017). Studies have found that local efficiency decreases linearly from adulthood to old age, while global efficiency remains unchanged. The PE method only considers the grade of the samples, not their metrics. As it is a sequential measure, the PE has some advantages over other commonly used entropy measures, including simplicity, low computational complexity without further model assumptions, and robustness in the presence of observed and dynamic noise. PE has been used in EEG signal studies of human absence epilepsy (Ferlazzo et al., 2014), typical absence seizures (Jing et al., 2014), and MCI (Timothy et al., 2014). These studies suggest that PE is a useful tool for studying brain complexity.

## 5 | CONCLUSION

In this study, a cohort of healthy subjects ranging from 6 to 85 years old was used to comprehensively analyze the whole brain and

separate networks from linear and quadratic perspectives using PE methods. We aimed to identify the global and network trajectories in the human brain during healthy aging to provide a complete description of the topological changes in the PE over time.

Overall, this study identified four basic aging trajectories, additional patterns with regard to developmental processes, and the differentiation of the brain during development. The four basic types of trajectories were as follows: a linear increase in the PE of a functional brain network; an early peak in the PE (<35 years); a PE peak in middle age (35–44 years); and a PE peak in older age (>44 years). These results suggest that the variations in lifespan trajectories could reflect associations between variation in entropy and brain development. These findings are important for elucidating methods to promote optimal healthy development and aging.

## 5.1 | Limitations

The limitation of this article is that, first, the data used in this study did not provide corresponding cognitive and behavioral characteristics. Therefore, we did not further explore whether the trajectories of the motor and neuropsychological scores were correlated with PE trajectories across age groups. Second, a possible explanation for the difference in peak points is the partial volume effects at different ages. In existing brain network research, the same template is used from youth to old age; thus, the technical requirements are not met, and there is no corresponding brain map from each period. Third, data on a wide range of age groups are currently scarce; our results would be more convincing if they were obtained from multiple data sets. We will continue our research in the future.

## ACKNOWLEDGMENT

This project is supported by the National Natural Science Foundation of China (61873178, 61906130, 62176177) and Shanxi Province Basic Research Program (Free Exploration) Project (20210302123112, 20210302124550, 20210302123099).

## CONFLICT OF INTEREST

The authors declare no conflicts of interest. The funders of this study had no role in the design; the collection, analyses, or interpretation of data; the writing of the manuscript; or the decision to publish the results.

## AUTHOR CONTRIBUTIONS

Yan Niu and Jie Sun completed the experimental process and wrote the manuscript. Xin Wen and Yanli Yang provided advice and guidance on the article. Bin Wang and Jie Xiang revised the manuscript content. Jie Xiang provided the direction and ideas of the research.

## DATA AVAILABILITY STATEMENT

The data that support the findings of this study are openly available in the Nathan Kline Institute (NKI, NY) and publicly available at the

International Neuroimaging Data-sharing Initiative (INDI) online ([http://fcon\\_1000.projects.nitrc.org/indi/enhanced/mri\\_protocol.html](http://fcon_1000.projects.nitrc.org/indi/enhanced/mri_protocol.html)).

## ORCID

Jie Sun  <https://orcid.org/0000-0002-6470-9452>

Bin Wang  <https://orcid.org/0000-0001-7771-5360>

## REFERENCES

- Achard, S., & Bullmore, E. (2007). Efficiency and cost of economical brain functional networks. *PLoS Computational Biology*, 3(2), e17.
- Allen, J. S., Bruss, J., Brown, C. K., & Damasio, H. (2005). Normal neuroanatomical variation due to age: The major lobes and a parcellation of the temporal region. *Neurobiology of Aging*, 26(9), 1245–1260 discussion 1279–1282.
- Bandt, C., & Pompe, B. (2002). Permutation entropy: A natural complexity measure for time series. *Physical Review Letters*, 88(17), 174102.
- Chen, M. L., Fu, D., Boger, J., & Jiang, N. (2019). Age-related changes in Vibro-tactile EEG response and its implications in BCI applications: A comparison between older and younger populations. *IEEE Transactions on Neural Systems and Rehabilitation Engineering*, 27(4), 603–610.
- Djma, B., Ijb, C., Ab, D., Ggp, B., Nkca, E., & Awsa, E. (2012). Diffusion tensor imaging of cerebral white matter integrity in cognitive aging. *Biochimica et Biophysica Acta (BBA) - Molecular Basis of Disease*, 1822(3), 386–400.
- Ferlazzo, E., Mammone, N., Cianci, V., Gasparini, S., Gambardella, A., Labate, A., Latella, M. A., Sofia, V., Elia, M., & Morabito, F. C. (2014). Permutation entropy of scalp EEG: A tool to investigate epilepsies. *Clinical Neurophysiology Official Journal of the International Federation of Clinical Neurophysiology*, 125(1), 13–20.
- Fjell, A. M., & Walhovd, K. B. (2010). Structural brain changes in aging: Courses, causes and cognitive consequences. *Reviews in the Neurosciences*, 21(3), 187–222.
- Fjell, A. M., Westlye, L. T., Grydeland, H. K., Amlien, I., Espeseth, T., Reinvang, I., Raz, N., Holland, D., Dale, A. M., & Walhovd, K. B. (2013). Critical ages in the life course of the adult brain: Nonlinear subcortical aging. *Neurobiology of Aging*, 34(10), 2239–2247.
- Giedd, J. N., Blumenthal, J., Jeffries, N. O., Castellanos, F. X., & Rapoport, J. L. (1999). Brain development during childhood and adolescence: A longitudinal MRI study. *Nature Neuroscience*, 2(10), 861–863.
- Giorgio, A., Watkins, K. E., Douaud, G., James, A. C., James, S., Stefano, N. D., Matthews, P. M., Smith, S. M., & Johansen-Berg, H. (2008). Changes in white matter microstructure during adolescence. *NeuroImage*, 39(1), 52–61.
- Goodro, M., Sameti, M., Patenaude, B., & Fein, G. (2012). Age effect on subcortical structures in healthy adults. *Psychiatry Research*, 203(1), 38–45.
- Gutchess, A. (2014). Plasticity of the aging brain: New directions in cognitive neuroscience. *Science*, 346(6209), 579–582.
- Hasan, K. M., Iftikhar, A., Kamali, A., Kramer, L. A., Ashtari, M., Cirino, P. T., Papanicolaou, A. C., Fletcher, J. M., & Ewing-Cobbs, L. (2009). Development and aging of the healthy human brain uncinate fasciculus across the lifespan using diffusion tensor tractography. *Brain Research*, 1276, 67–76.
- Heuninckx, S., Wenderoth, N., & Swinnen, S. P. (2008). Systems neuroplasticity in the aging brain: Recruiting additional neural resources for successful motor performance in elderly persons. *Journal of Neuroscience*, 28(1), 91–99.
- Hoffmann, M. (2020). Right dominant Frontoparietal network for spatial orientation (dorsal attention and visuospatial attention). *Clinical Mentation Evaluation*.
- Huttenlocher, P. R. (1990). Morphometric study of human cerebral cortex development. *Neuropsychologia*, 28(6), 517–527.

- Jeza, C., Aaaa, B., Ct, D., Amg, B., & Ot, E. (2020). HGC: HyperGraph based clustering scheme for power aware wireless sensor networks - ScienceDirect. *Future Generation Computer Systems*, 105, 175–183.
- Jing, L., Jiaqing, Y., Xianzeng, L., & Gaoxiang, O. (2014). Using permutation entropy to measure the changes in EEG signals during absence seizures. *Entropy*, 16(6), 3049.
- Karl, N., Sarah, T., Richard, C., Wayne, M., & Christian, B. (2017). Evolution of deep gray matter volume across the human lifespan. *Human Brain Mapping*, 38(8), 3771–3790.
- Kochunov, P., Williamson, D. E., Lancaster, J., Fox, P., & Glahn, D. C. (2012). Fractional anisotropy of water diffusion in cerebral white matter across the lifespan. *Neurobiology of Aging*, 33(1), 9–20.
- Lebel, C., Walker, L., Leemans, A., Phillips, L., & Beaulieu, C. (2008). Microstructural maturation of the human brain from childhood to adulthood. *NeuroImage*, 40(3), 1044–1055.
- Lindbergh, C. A., Zhao, Y., Lv, J., Mewborn, C. M., Puente, A. N., Terry, D. P., Renzi-Hammond, L. M., Hammond, B. R., Liu, T., & Miller, L. S. (2019). Intelligence moderates the relation between age and inter-connectivity of resting state networks in older adults. *Neurobiology of Aging*, 78, 121.
- Liu, J., Xu, P., Zhang, J., Jiang, N., Li, X., & Luo, Y. (2019). Ventral attention-network effective connectivity predicts individual differences in adolescent depression. *Journal of Affective Disorders*, 252, 55–59.
- Liu, T., Yan, Y., Ai, J., Chen, D., Wu, J., Fang, B., & Yan, T. (2021). Disrupted rich-club organization of brain structural networks in Parkinson's disease. *Brain Structure and Function*, 49, 1–13.
- Lupien, S. J., Evans, A., Lord, C., Miles, J., Pruessner, M., Pike, B., & Pruessner, J. C. (2007). Hippocampal volume is as variable in young as in older adults: Implications for the notion of hippocampal atrophy in humans. *NeuroImage*, 34(2), 479–485.
- Müller-Oehring, E. M., Schulte, T., Rohlfing, T., Pfefferbaum, A., & Sullivan, E. V. (2013). Visual search and the aging brain: Discerning the effects of age-related brain volume shrinkage on alertness, feature binding, and attentional control. *Neuropsychology*, 27(1), 48–59.
- Ostby, Y., Tamnes, C. K., Fjell, A. M., Westlye, L. T., Due-Tønnessen, P., & Walhovd, K. B. (2009). Heterogeneity in subcortical brain development: A structural magnetic resonance imaging study of brain maturation from 8 to 30 years. *The Journal of Neuroscience: The Official Journal of the Society for Neuroscience*, 29(38), 11772.
- Potvin, O., Mouiha, A., Dieumegarde, L., & Duchesne, S. (2016). Normative data for subcortical regional volumes over the lifetime of the adult human brain. *NeuroImage*, 137, 9–20.
- Power, J. D., Cohen, A. L., Nelson, S. M., Wig, G. S., & Petersen, S. E. (2011). Functional network organization of the human brain. *Neuron*, 72(4), 665–678.
- Salthouse, T. A. (2009). When does age-related cognitive decline begin? *Neurobiology of Aging*, 30(4), 507–514.
- Shumbayawonda, E., López-Sanz, D., Brua, R., et al. (2019). Complexity changes in preclinical Alzheimer's disease: An MEG study of subjective cognitive decline and mild cognitive impairment [J]. *Clinical Neurophysiology*, 131(2).
- Smits, F. M., Porcaro, C., Cottone, C., Cancelli, A., & Tecchio, F. (2016). Electroencephalographic fractal dimension in healthy ageing and Alzheimer's disease. *PLoS One*, 11(2), 1–16.
- Sokumbi, M. O., Cameron, G. G., Ahearn, T. S., Murray, A. D., & Staff RT. (2015). Fuzzy approximate entropy analysis of resting state fMRI signal complexity across the adult life span. *Medical Engineering & Physics*, 37(11), 1082–1090.
- Sokumbi, M. O., Fung, W., Sawlani, V., Choppin, S., Linden, D. E. J., & Thome, J. (2013). Resting state fMRI entropy probes complexity of brain activity in adults with ADHD. *Psychiatry Research: Neuroimaging*, 214(3), 341–348.
- Song, X. W., Dong, Z. Y., Long, X. Y., Li, S. F., Zuo, X. N., Zhu, C. Z., He, Y., Yan, C. G., Zang, Y. F., & Harrison, B. J. (2011). REST: A toolkit for resting-state functional magnetic resonance imaging data processing. *PLoS One*, 6, e25031.
- Sowell, E. R., Peterson, B. S., Thompson, P. M., Welcome, S. E., Henkenius, A. L., & Toga, A. W. (2003). Mapping cortical change across the human life span. *Nature Neuroscience*, 6(3), 309–315.
- Sun, J., Wang, B., Niu, Y., Tan, Y., & Xiang, J. (2020). Complexity analysis of EEG, MEG, and fMRI in mild cognitive impairment and Alzheimer's disease: A review. *Entropy*, 22(2), 239.
- Timothy, L. T., Krishna, B. M., Menon, M. K., & Nair, U. (2014). *Permutation entropy analysis of EEG of mild cognitive impairment patients during memory activation task*. Springer International Publishing.
- Touroutoglou, A., Zhang, J., Andreano, J. M., Dickerson, B. C., & Barrett, L. F. (2018). Dissociable effects of aging on salience sub-network connectivity mediate age-related changes in executive function and affect. *Frontiers in Aging Neuroscience*, 10, 410.
- Walhovd, K. B., Westlye, L. T., Amlie, I., Espeseth, T., Reinvang, I., Raz, N., Agartz, I., Salat, D. H., Greve, D. N., & Fischl, B. (2011). Consistent neuroanatomical age-related volume differences across multiple samples. *Neurobiology of Aging*, 32(5), 916–932.
- Wang, C., Kang, M., Li, Z., Li, Y., & Xu, J. (2020). Altered relation of resting-state alpha rhythm with blood oxygen level dependent signal in healthy aging: Evidence by EEG-fMRI fusion analysis. *Clinical Neurophysiology*, 131(9), 2105–2114.
- Yan, C., & Zang, Y. (2010). DPARSF: A MATLAB toolbox for "pipeline" data analysis of resting-state fMRI. *Frontiers in Systems Neuroscience*, 4(13), 43.
- Yan, T., Wang, W., Yang, L., Chen, K., Rong, C., & Ying, H. (2018). Rich club disturbances of the human connectome from subjective cognitive decline to Alzheimer's disease. *Theranostics*, 8(12), 3237–3255.
- Yang, L., Yan, Y., Wang, Y., Hu, X., Lu, J., Chan, P., Yan, T., & Han, Y. (2018). Gradual disturbances of the amplitude of low-frequency fluctuations (ALFF) and fractional ALFF in Alzheimer Spectrum. *Frontiers in Neuroscience*, 12, 975.
- Yeatman, J. D., Wandell, B. A., & Mezer, A. A. (2014). Lifespan maturation and degeneration of human brain white matter. *Nature Communications*, 5, 4932.
- Zhao, T., Cao, M., Zuo, X. N., Dong, Q., He, Y., & Shu, N. (2015). Age-related changes in the topological Organization of the White Matter Structural Connectome across the human lifespan. *Human Brain Mapping*, 47, 26–27.
- Zhao, T., Sheng, C., Bi, Q., Niu, W., Shu, N., & Han, Y. (2017). Age-related differences in the topological efficiency of the brain structural connectome in amnesic mild cognitive impairment. *Neurobiology of Aging*, 59, S0197458017302609.
- Zhixiong, Y., Xun, L., Shuping, T., Yunlong, T., Gaoxia, W., Zhi, Y., & Xinian, Z. (2016). Developmental cognitive neuroscience: Functional connectomics agenda for human brain lifespan development. *Chinese Science Bulletin*, 61, 718–727.

**How to cite this article:** Niu, Y., Sun, J., Wang, B., Yang, Y., Wen, X., & Xiang, J. (2022). Trajectories of brain entropy across lifetime estimated by resting state functional magnetic resonance imaging. *Human Brain Mapping*, 43(14), 4359–4369. <https://doi.org/10.1002/hbm.25959>